Discrete breathers in dc-biased Josephson-junction arrays

J. J. Mazo
Department of Electrical Engineering and Computer Science, Massachusetts Institute of Technology, Cambridge, Massachusetts 02139 and Departamento de Física de la Materia Condensada and ICMA, CSIC–Universidad de Zaragoza, E-50009 Zaragoza, Spain

E. Trías and T. P. Orlando
Department of Electrical Engineering and Computer Science, Massachusetts Institute of Technology, Cambridge, Massachusetts 02139
(Received 7 December 1998)

We propose a method to excite and detect a rotor localized mode (rotobreather) in a Josephson-junction array biased by dc currents. In our numerical studies of the dynamics we have used experimentally realizable parameters and included self-inductances. We have uncovered two families of rotobreathers. Both types are stable under thermal fluctuations and exist for a broad range of array parameters and sizes including arrays as small as a single plaquette. We suggest a single Josephson-junction plaquette as an ideal system to experimentally investigate these solutions. [S0163-1829(99)02821-0]

The phenomenon of intrinsic localization [intrinsic localized modes or discrete breathers (DB)] is a recent discovery in the subject of nonlinear dynamics.[1] DB are solutions to the dynamics of discrete extended systems for which energy is exponentially localized in space. They appear either as oscillator localized modes, for which a localized group of oscillators librate, or rotor localized modes or rotobreathers, for which a group of oscillators rotate while the others librate.[2] Recently, it has been found that DB are not restricted to periodic solutions but can also include more complex (chaotic) dynamics.[3]

DB have been proven to be generic solutions in Hamiltonian[4] and dissipative[5] nonlinear lattices. It is believed that they might play an important role in the dynamics of a large number of systems, such as coupled nonlinear oscillators or rotors.

Though intrinsic localized modes have been the object of great theoretical and numerical attention in the last ten years, they have yet to be generated and detected in an experiment. Thus finding the best system and method for the generation, detection, and study of an intrinsic localized mode in a condensed-matter system has become an important challenge.[6,7]

Josephson-junctions (JJ) arrays are excellent experimental systems for studying nonlinear dynamics.[8] In this paper we propose an experiment to detect a rotating localized mode in JJ anisotropic ladder arrays biased by dc external currents.[9] For this, we have done numerical simulations of the dynamics of an open ladder including induced fields[10] at experimentally accessible values of the parameters of the array. We also propose a method for exciting a rotobreather in the array. We distinguish between two families of solutions which present different voltage patterns in the array. Both types are robust to random fluctuations and exist over a range of parameter values and array sizes. Unexpectedly, we have found that many of the rotobreather solutions do not satisfy the up-down symmetry usually assumed for most types of dynamical solutions in the ladder. We also show that a DB solution can be most readily studied in a single plaquette.

According to the resistively and capacitively shunted junction (RCSJ) model, a Josephson junction is characterized by its critical current I_c, normal-state resistance R_n, and capacitance C. The junction voltage v is related to the gauge-invariant phase difference φ as

$$v = \frac{\Phi_0}{2\pi}\frac{d\varphi}{dt}, \tag{1}$$

where Φ_0 is the flux quantum. After standard rescaling of the time by $\tau = \sqrt{\Phi_0 C/2\pi I_c}$, the normalized current through the junction is

$$i = \ddot{\varphi} + \Gamma\dot{\varphi} + \sin\varphi; \tag{2}$$

here Γ represents a damping and is directly related to the Stewart-McCumber parameter $\beta_c = \Gamma^{-2} = 2\pi I_c C R_n^2/\Phi_0$.

Our anisotropic JJ ladders (see Fig. 1) contain junctions of two different critical currents: I_{ch} for the horizontal junctions and I_{cv} for the vertical ones. Anisotropic arrays are easily fabricated by varying the area of the junctions. In the case of unshunted junctions, the critical current and capacitance are proportional to this area. Due to the constant $I_c R_n$ product, the normal-state resistance is inversely proportional to the junction area. The anisotropy parameter h can then be defined as $h = I_{ch}/I_{cv} = C_h/C_v = R_v/R_h$.

To write the governing equations of an anisotropic JJ ladder array with N cells, Fig. 1, we need to apply current con-

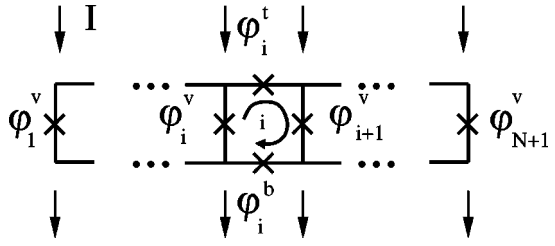

FIG. 1. Anisotropic ladder array with uniform current injection. Vertical junctions have critical current I_{cv} and horizontal junctions I_{ch}.

servation at each node and flux quantization at each mesh. We are including self-induced magnetic fields so that flux quantization at mesh j yields

$$(\nabla\times\varphi)_j=-2\pi f_j. \tag{3}$$

Here $(\nabla\times\varphi)_j=\varphi_j^t+\varphi_{j+1}^v-\varphi_j^b-\varphi_j^v$ and it represents the circulation of gauge-invariant phase differences in mesh $j=1$ through N. The self-induced flux through mesh j normalized by Φ_0 is given by f_j. The resulting equations can be written compactly as

$$h(\ddot{\varphi}_j^t+\Gamma\dot{\varphi}_j^t+\sin\varphi_j^t)=-\lambda(\nabla\times\varphi)_j$$

$$\ddot{\varphi}_j^v+\Gamma\dot{\varphi}_j^v+\sin\varphi_j^v=\lambda[(\nabla\times\varphi)_j-(\nabla\times\varphi)_{j-1}]+I$$

$$h(\ddot{\varphi}_j^b+\Gamma\dot{\varphi}_j^b+\sin\varphi_j^b)=\lambda(\nabla\times\varphi)_j, \tag{4}$$

where the open boundaries can be imposed by setting $(\nabla\times\varphi)_0=(\nabla\times\varphi)_{N+1}=0$ in Eqs. (4). The system has four independent parameters: h, Γ, the penetration depth $\lambda=\Phi_0/2\pi I_{cv}L$, where L is the mesh self-inductance, and the normalized external current I. On writing Eqs. (3) and (4) we assume zero external field and normalize by I_{cv}. Nonzero external fields can be included in the model replacing the $(\nabla\times\varphi)_j$ terms in Eqs. (3) and (4) by $(\nabla\times\varphi)_j+2\pi f_j^{ext}$ where f_j^{ext} is the flux due to an applied external field, measured in terms of Φ_0.

The parameter values we will consider are based on Nb-Al_2O_x-Nb junctions with a critical current density of 1000 A/cm^2. Typical values of the Stewart-McCumber parameter and the penetration depth for arrays with $h=1/4$ are $\beta_c\sim 30$ and $\lambda\sim 0.02$. For the purposes of this work we will let $\Gamma=0.2$, $\lambda=0.02$, and $N=8$.

Consider the $h=0$ limit in Eqs. (4). In this limit the vertical junctions behave as uncoupled damped pendula driven by an external current I. There, we can think of a configuration in which one or a few of the phases are rotating or oscillating around their equilibrium points while the others remain at rest. Thus rotor and/or oscillator localized modes appear as solutions to the dynamics when the array is biased either by dc or ac external currents.

For a single underdamped junction driven by a constant external current, the response measured in terms of dc voltage presents a hysteresis loop between the depinning and the retrapping currents. In this range the pinned $(V=0)$ and rotating $(V\neq 0)$ solutions coexist. Then the rotobreather solution in the $h=0$ limit corresponds to a solution in which the phase of one of the vertical junctions is rotating while the other vertical junctions are at rest.

As h is increased from zero the nonconvex character of the coupling allows for the continued existence of rotobreathers in the system. Since a solution with a time increasing field cannot physically exist, the flux quantization condition [Eq. (3)] implies that each cell with a rotating junction must have at least one other junction which is rotating. Thus for the single rotobreather solution one of the vertical and some of the horizontal neighboring junctions rotate. Figure 2 shows schematically simple rotating localized modes in a ladder and in the single plaquette. These DB are amenable to simple experimental detection when measuring the average voltage through different junctions.

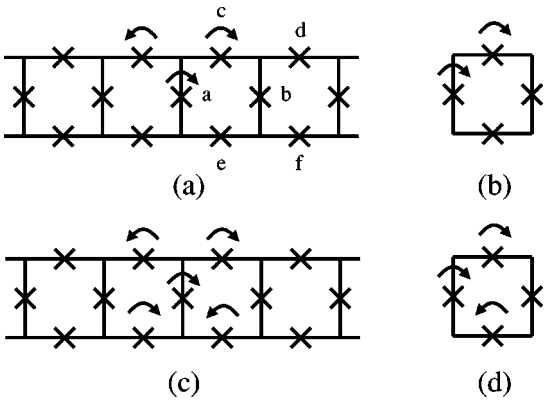

FIG. 2. Schematic picture of rotobreather solutions: type-A rotobreather in the ladder array (a) and plaquette (b); type-B rotobreather in the ladder (c) and plaquette (d). Arrows are associated with rotating junctions and labels in (a) corresponds to graphs in Fig. 3.

Although the rotobreather solution can theoretically be continued from its $h=0$ limit by varying h, we have developed a simple method of exciting it in an array. This method should be experimentally reproducible and has three steps: (i) bias all the array up to the operating point $(I=I^*)$; (ii) increase the current injected into one of the junctions to a value of the current above the junction critical current $(I=I^*+\tilde{I}>1)$; (iii) go back to the operating point by decreasing to zero the value of this extra current $\tilde{I}$. Typical values of I^* and $\tilde{I}$ in our simulations are 0.6.

We have checked the robustness of this method under fluctuations by simulating the equations of the ladder while adding a noise current to the junctions (this is the standard manner of including thermal effects in the system[11]). Thus we are able to excite DB in the ladder at some values of the parameters of the system. The solution showed in Fig. 3 was excited using this procedure.

Henceforth, we are going to consider ladders with an even number of cells for which one vertical junction (the central one) is rotating. We will relabel this junction as $j=0$.

Figure 3 shows a solution of a stable rotobreather in a JJ ladder. We plot the phase portrait $(\varphi_j^q,\ \dot{\varphi}_j^q)$ of some of the superconducting gauge invariant phase differences of the array. The corresponding junctions are shown in Fig. 2(a). For clarity we have reduced the values of the phases to the $(-\pi,\pi]$ interval. We see that at this value of the penetration depth the solution is highly localized, while three of the junctions describe a nearly sinusoidal rotation, all the others oscillate with decreasing amplitudes. The average voltage through the three rotating junctions in the array is different from zero and equals to zero for all the other junctions. Figure 4 shows the average value of the induced field of the cells of the array. It decreases exponentially as $\overline{f_j}\sim e^{-j/0.26}$ $(j\geq 0$ and $f_{-j}=-f_{j-1})$.

There are some surprising characteristics in this solution. Current conservation in the open ladder implies $i_j^t=-i_j^b$. From Eqs. (2) and (4) we can see that $\varphi_j^t=-\varphi_j^b$ is a simple solution of the dynamics of the array and it corresponds to the up-down symmetry of the phases. All the previous theo-

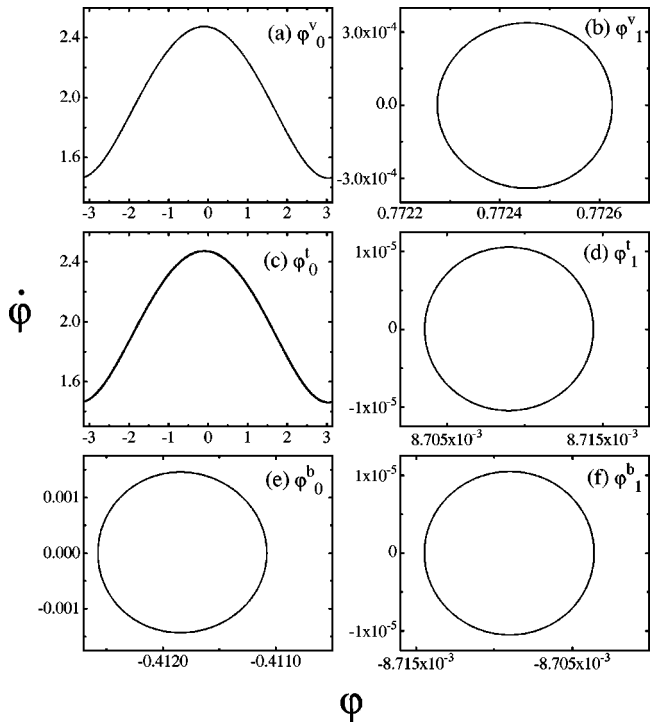

FIG. 3. Example of a rotobreather in an eight-cell JJ ladder at $h=0.25$, $\lambda=0.02$; $\Gamma=0.2$ and $I_{dc}=0.6$. The only vertical rotating junction is the central one, $j=0$, and we show the phase portrait of six of the phases of the array: (a) φ_0^v, (b) φ_1^v, (c) φ_0^t, (d) φ_1^t, (e) φ_0^b, and (f) φ_1^b. The plotted phases are labeled in Fig. 2(a). Also, in this case $\varphi_j^v=\varphi_{-j}^v$, $\varphi_{-j}^{t(b)}=-\varphi_{j-1}^{t(b)}$.

retical approaches to the dynamics of the array (which include whirling modes, resonances, row switching, etc.) and many of the numerical ones focus on solutions which satisfy this up-down symmetry. However, looking at Fig. 3 we see that the rotobreather solution shown there does not comply with this simple symmetry; that is, $\varphi_j^t \neq -\varphi_j^b$ although $i_j^t=-i_j^b$.

We will distinguish between two families of single rotobreather solutions in the ladder which present different voltage patterns. The first family, rotobreather A [see Fig. 2(a)], is characterized by one vertical and two horizontal rotating junctions. Type-A solutions have two possible configurations. The two rotating horizontal junctions can be both in the same side, either top or bottom, as in Fig. 2(a); or one in the top and the other in the bottom. The second family, rotobreather B [Fig. 2(c)], is characterized by one vertical and four horizontal rotating junctions. The solution shown in Figs. 3 and 4 is a type A rotobreather. Up-down symmetric solutions belong to family B, but not all family-B solutions satisfy this symmetry.

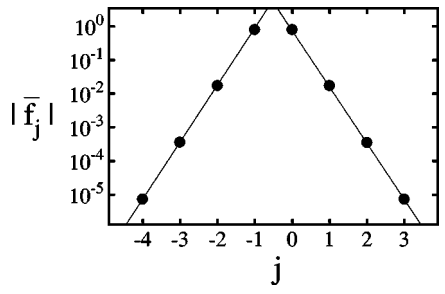

FIG. 4. The average value of the induced flux ($f_{-j}=-f_{j-1}$) at all the cells of the ladder for the rotobreather shown in Fig. 3. This average value decreases exponentially which is characteristic of DB solutions.

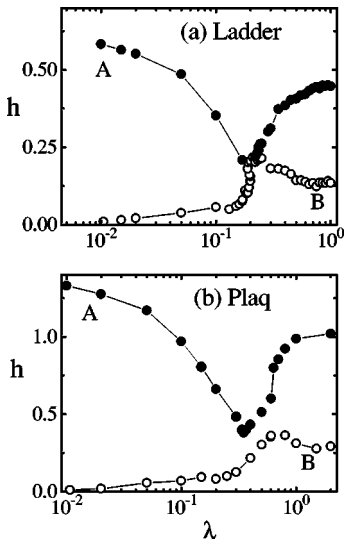

FIG. 5. Maximum values of anisotropy for the existence of type-A (solid circles) and type-B (open circles) rotobreather solutions at different values of λ in an eight-cell ladder (a) and a single plaquette array (b). Γ and I are equal to 0.2 and 0.6, respectively. Lines serve as a guide to the eyes.

Figures 3 and 4 show a solution for which the scale of localization is smaller than one cell. Thus it is natural to study the DB solution in the simplest ladder array, the single plaquette. Obviously, the concept of exponential spatial localization is not applicable to the plaquette, but all the other characteristics of the solution remain. In particular we will also distinguish between type-A and type-B rotobreather solutions in the plaquette, which in this case correspond to one vertical and one horizontal rotating junctions [Fig. 2(b)], and one vertical and both horizontal rotating junctions [Fig. 2(d)], respectively. The single plaquette biased by dc external currents, is then proposed as the simplest and most convenient experimental system for detecting a rotating localized mode. The method for exciting the mode is also applicable to this system.

An important experimental issue then becomes finding the region of existence of these DB solutions with respect to the system parameters in order to investigate the feasibility of designing an array to detect a DB. To design an array we need to calculate the junction areas, so that the anisotropy needs to be known. Since different values of the anisotropy affect the cell geometry, they also change the value of λ. On the other hand, Γ is determined by the current density of the junctions and therefore it is fixed and independent of the geometry while the applied current can be easily changed while measuring. In order to make an optimal design we will fix the value of I and Γ to 0.6 and 0.2, respectively, and study DB solutions in the (h-λ) plane of parameters.

Type-A and type-B rotobreathers exist close to the $h=0$ limit. We then calculate the maximum value of the anisotropy for which a DB exists as a stable solution of the dynamical equations for different values of λ. Figures 5(a) and

(b) show the result for the ladder and the single plaquette. The data were calculated by integrating the equations of motion for the corresponding system with a small quantity of noise. We start with a type-B rotobreather and $h \sim 0.001$. As we increase h, type-B solutions become unstable and the solution evolves to a type-A rotobreather. As we further increase h this rotobreather becomes unstable and the system usually jumps to either a pinned or a whirling state. To verify that our method is accurate, we have calculated Floquet multipliers for periodic rotobreather solutions and found results consistent with those shown in Fig. 5.

We note that when doing this existence analysis of the solutions we find many different single-breather solutions. Most are periodic with different periods and amplitudes but there are some that appear to be chaotic [specially close to the $\lambda = 0.2$ region in Fig. 5(a)]. A detailed study of the different bifurcations which include period doubling bifurcations to chaos is in current progress. There also exists a large family of different multibreather solutions, each one with its own domain of existence.

Figure 5 shows that at $\Gamma = 0.2$ and $I = 0.6$ type-A solutions exist at larger values of the anisotropy than type-B solutions. Also a simple inspection reveals a strong similarity between Figs. 5(a) and 5(b). The similarity can be easily understood. The rotobreather solution shown in Figs. 3 and 4 presents a mirror symmetry with respect to the rotating vertical junction: $\varphi_j^v = \varphi_{-j}^v$, and $\varphi_{-j}^{t(b)} = -\varphi_{j-1}^{t(b)}$. In the case of solutions satisfying a mirror symmetry it is possible to map the dynamics of a JJ ladder for which the rotating junction is the central one, to the dynamics of a smaller JJ ladder for which the rotating junction is on one of the ends. Then, due to the localized nature of the DB solution, the dynamics can be approximated by studying a single plaquette. When doing these transformations we need to rescale two of the parameters of the equations. Thus results for the DB solution studied above present some similarities with the dynamics of a DB in a single plaquette when $h_p = 2h_l$ and $\lambda_p = 2\lambda_l$. By establishing a criteria for the design of simple experiments to detect these intrinsic localized modes we hope to stimulate experimental investigations.

The research was supported in part by NSF Grant No. DMR-9610042 and DGES (PB95-0797). J. J. M. thanks the Fulbright commission and the MEC (Spain) for financial support. We thank A. E. Duwel, F. Falo, L. M. Floría, P. J. Martínez, and S. H. Strogatz for useful discussions.

[1] A.J. Sievers and S. Takeno, Phys. Rev. Lett. **61**, 970 (1988); for a recent review, see Physica D **113** Issue 2-4 (1998) and Physica D **119** Issue 1-2 (1998).

[2] S. Takeno and M. Peyrard, Physica D **92**, 140 (1996); Phys. Rev. E **55**, 1922 (1997).

[3] P.J. Martínez, L.M. Floría, F. Falo, and J.J. Mazo, Europhys. Lett. **45**, 444 (1999); D. Bonart and J.B. Page (unpublished).

[4] R.S. MacKay and S. Aubry, Nonlinearity **7**, 1623 (1994).

[5] J.-A. Sepulchre and R.S. MacKay, Nonlinearity **10**, 679 (1997).

[6] L.M. Floría, J.L. Marín, P.J. Martínez, F. Falo, and S. Aubry, Europhys. Lett. **36**, 539 (1996); L.M. Floría, J.L. Marín, S. Aubry, P.J. Martínez, F. Falo, and J.J. Mazo, Physica D **113**, 387 (1998); P.J. Martínez, L.M. Floría, J.L. Marín, S. Aubry, and J.J. Mazo, *ibid.* **119**, 175 (1998).

[7] R. Lai and A.J. Sievers, Phys. Rev. Lett. **81**, 1937 (1998).

[8] S. Watanabe, H.S.J. van der Zant, S.H. Strogatz, and T.P. Orlando, Physica D **97**, 429 (1996); J.C. Ciria, and C. Giovannella, J. Phys.: Condens. Matter **10**, 1453 (1998).

[9] This system has recently been proposed (Ref. 6) as a good candidate to experimentally detect a discrete breather when biased by ac currents. But, generating the rotobreather and the high frequencies involved in the drive are serious obstacles towards an experimental detection in this ac case. Regarding the dc case, the existence of these modes in coupled rotor systems has been proved by R.S. MacKay, and J.-A. Sepulchre, Physica D **119**, 148 (1998), and numerically found by Z. Zheng, B. Hu, and G. Hu, Phys. Rev. E **57**, 1139 (1998).

[10] The inclusion of induced magnetic fields has been shown to be important for understanding some experimental results in E. Trías, H.S.J. van der Zant, and T.P. Orlando, Phys. Rev. B **54**, 6568 (1996); H.R. Shea, M.A. Itzler, and M. Tinkham, *ibid.* **51**, 12 690 (1995).

[11] V. Ambegaokar, and B.I. Halperin, Phys. Rev. Lett. **22**, 1364 (1969).